Macromolecules **2006,** *39,* 6327−6330

Compression-Induced Hierarchical Nanostructures of a Poly(ethylene oxide)-*block*-Dendronized Polymethacrylate Copolymer at the Air/Water Interface

Cai-Xia Cheng,[†] Ti-Feng Jiao,[‡] Ru-Pei Tang,[†]
Er-Qiang Chen,*[,§] Ming-Hua Liu,*[,‡] and Fu Xi*[,†]

State Key Laboratory of Polymer Physics and Chemistry,
Institute of Chemistry, The Chinese Academy of Science,
Beijing 100080, China; CAS Key Laboratory of Colloid and
Interface Science, Institute of Chemistry, The Chinese
Academy of Science, Beijing 100080, China; and
Department of Polymer Science and Engineering and
The Key Laboratory of Polymer Chemistry and Physics of
Ministry of Education, College of Chemistry and Molecular
Engineering, Peking University, Beijing 100871, China

Received June 28, 2006
Revised Manuscript Received August 4, 2006

Amphiphilic block copolymers (ABCs) are of great interest not only with regard to the fundamental issues of their self-assembly but also for the properties amenable to practical applications such as biological mimics, drug delivery, and nanostructured materials.[1−5] At the air/water interface, ABCs are able to form surface micelles,[6] which are usually circular, rod, and planar in shape, analogous to the spherical, cylindrical, and lamellar micelles in solutions, respectively.[7] Various mechanisms of surface micelle formation have been proposed: (1) From a thermodynamic point of view, the discrete amphiphilic molecules at the air/water interface assemble to micelles only when the surface concentration exceeds a critical micelle concentration.[8] Therefore, during the use of a Langmuir−Blodgett (LB) trough, surface micelles can be compression-induced.[9] (2) Competition between film spreading and polymer entanglement resulting from solvent evaporation determines a surface micelle formation.[10] (3) Surface micelles are formed spontaneously when solutions are spread on water surface, and this process is neither compression nor spreading solvent dependent.[6,7,11−13]

We consider that the chemical structures and molecular architectures of polymers dominate the intermolecular interactions and packing density and further determine many of the LB film properties, the phases which are formed, and the rates at which transitions between phases occur. The surface micelle morphology is highly dependent on the degree of polymerization (DP), composition, and molecular architecture of ABC molecules. Recently, inspired by the works on dendronized polymers that are significantly shape persistent,[14,15] we have synthesized a new type of ABC containing the hydrophilic block of poly(ethylene oxide) (PEO) and the hydrophobic block of dendronized linear polymethacrylate (PDMA).[16] Compared with ABCs that are commonly coil−coil, our polymers are coil−semirod. In this Communication, we describe the phase transitions and morphology evolution at the air/water interface of a PEO-*b*-PDMA. We have found that the sample could form wormlike surface micelles. Moreover, upon compression, the micelles can be close-packed with order in two dimensions (2D), twisted, and finally collapsed into unusual three-dimensional (3D) large aggregates that look like "spring" and "disk", showing a unique hierarchical nanostructure evolution.

Scheme 1. Chemical Structure of the PEO$_{45}$-*b*-PDMA$_{69}$

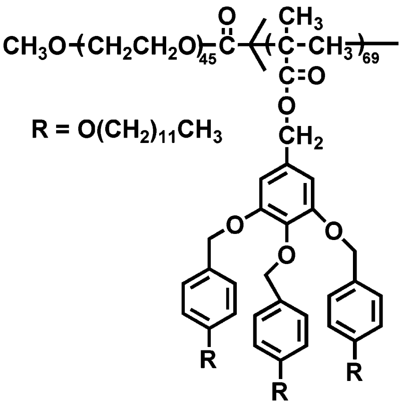

The diblock copolymer studied (PEO$_{45}$-*b*-PDMA$_{69}$, see Scheme 1) was synthesized via the atom transfer radical polymerization method (ATRP) of generation 1 (G1) Percec-type dendritic methacrylate using a PEO macroinitiator (see Supporting Information).[16] The polymer possesses the DPs of 45 and 69 for the PEO and PDMA blocks, respectively, and a polydispersity of 1.15. Our differential scanning calorimetry (DSC) experiments showed that the PEO$_{45}$-*b*-PDMA$_{69}$ only presented a glass transition at 44.5 °C, which is 8 °C lower than that of the homo-PDMA with a similar DP.[16a] For the entire temperature range from −50 to 150 °C, the crystallization/melting of the PEO block and the liquid crystal (LC) transition of PDMA[15] were not observed during DSC cooling and heating scans. In the wide-angle X-ray scattering (WAXS) experiments, the sample only presented an amorphous halo at the high 2θ region with a halo maximum corresponding to a *d* spacing of 0.45 nm. At the low 2θ region, a strong diffraction peak with the *d* spacing of 4.3 nm was observed, which should be associated with the average distance between two adjacent PDMA chains.[15] The absence of the higher order diffraction in the low 2θ region indicated no long-range ordered hexagonal columnar LC (Φ_H) phase of the PDMA blocks existed. The experimental results implied that the PEO and PDMA blocks were partially miscible.

The LB films of PEO$_{45}$-*b*-PDMA$_{69}$ were obtained with a KSV-1100 film balance system (KSV Instrument, Helsinki, Finland) by spreading the chloroform solutions (0.2 mg/mL) on the water surface. The temperature of the subphase was controlled to be 20.0 ± 0.2 °C. In each trial, 100 μL of the solution was added dropwise to the water surface at uniformly spaced locations across the surface. After waiting 30 min for solvent evaporation, the surface pressure−area (π−A) isotherms were measured by a symmetric compression with a constant barrier speed of 5 mm/min. The LB films of the copolymer were transferred onto hydrophobic silicon wafers at various molecular areas by a horizontal lifting method, starting from above the water surface with a typical vertical speed of 1 mm/min. The silicon wafers were first cleaned by an oxidizing mixture of HNO_3/H_2O_2 (1:2, v/v) and then rinsed several times in pure water. To make the substrates hydrophobic, the cleaned wafers were exposed to vapors of octadecyltrichlorosilane for

---

[†] State Key Laboratory of Polymer Physics and Chemistry, The Chinese Academy of Science.

[‡] CAS Key Laboratory of Colloid and Interface Science, The Chinese Academy of Science.

[§] Peking University.

* To whom the correspondence should be addressed. E-mail: eqchen@pku.edu.cn; liumh@iccas.ac.cn; xifu@iccas.ac.cn.

10.1021/ma0614500 CCC: $33.50

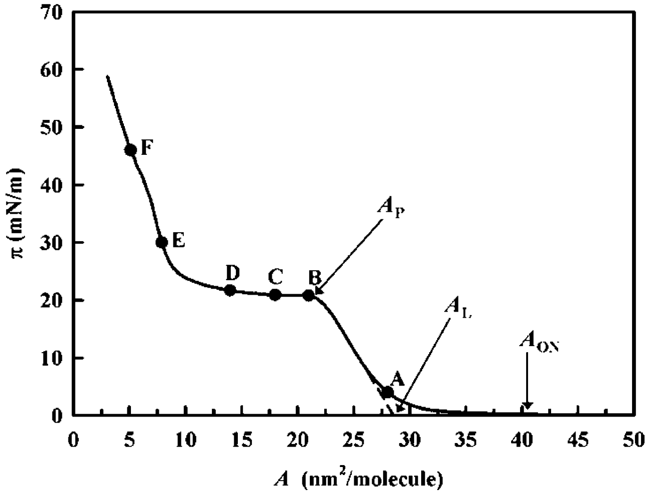

Figure 1. Surface pressure (π) vs area per molecule (A) at 20 °C for the LB film of PEO$_{45}$-*b*-PDMA$_{69}$. A_{ON}, A_L, and A_P are the molecular areas of the onset, limiting, and beginning of the plateau region, respectively.

2 h, heated to 100 °C in oven for 2 h, and then rinsed with chloroform. The SEM experiments were carried out with a Hitachi S-4300 microscope (15 kV, 10 μA). For morphology observation, the SEM samples were presputtered with a Pt layer. The energy-dispersive X-ray (EDX) microanalysis of the samples without Pt layer was obtained with an EDX detector installed on the SEM. The diameter of the selective microareas is 30 nm.

When the PEO$_{45}$-*b*-PDMA$_{69}$ dissolved in chloroform, which is a good solvent for both the PEO and PDMA blocks, was spread on the water surface, it formed a stable Langmuir film. As shown by Figure 1, the $\pi - A$ isotherm initially displays a phase with nearly zero spreading pressure, followed by a rise in π. Taking +0.2 mN/m above the baseline as the onset, the corresponding onset area (A_{ON}) is about 42 nm^2/molecule. The π gradually increases and reaches a plateau region at 21 nm^2/molecule (A_P). For this first increase in π, extrapolating the maximum slope of the isotherm to $\pi = 0$ axis gives a limiting area (A_L) of 28.6 nm^2/molecule. The plateau region keeps a π of ~21 mN/m and ends at 12 nm^2/molecule. A further compression leads to a second increase in π, which is much more abrupt than the first one, indicating that the film became rather incompressible. Within this second π increase, an obscure inflection point at nearly 42 mN/m is observed.

The shape of isotherm for the sample (Figure 1) looks similar to those of PEO anchored by some hydrophobic moieties described in the literature.[10a,12,13,17] However, our morphology observations reveal that the interfacial behavior of the coil–semirod PEO$_{45}$-*b*-PDMA$_{69}$ is quite different from those reported. Figure 2 illustrates a set of SEM images of the LB films corresponding to the points A–F in Figure 1. While the LB films transferred from the air/water interface at $\pi \approx 0$ were featureless, wormlike surface micelles were observed after the first increase in π. In Figure 2A at 28 nm^2/molcecule, the width of the wormlike micelles is measured to be 45–55 nm. Some areas in vicinity to the micelles look empty, which should arise from the depletion of molecules; some others are rough and should be covered by the molecules that tend to assemble. When further compressed to 21 nm^2/molecule (A_P in Figure 1), the micelles are arrayed with order in 2D, and their long axis is nearly perpendicular to the compression direction (see Figure 2B). This pattern indicates that the wormlike micelles are rather flexible and, if under compression, can be extended to accommodate the reduced surface area. Nevertheless, at this stage, the 2D close packing seems not to alter the inner structure of the micelles. The periodicity of the ordered structure, i.e., the micelle width, is ~50 nm, agreeing with the size of the discrete micelles shown in Figure 2A. At the A_p of 21 nm^2/molecule, the aggregation number of the wormlike micelles with the width of ~50 nm is calculated to be ~2.5 diblock molecules/nm of length.[7a,18] Assuming that the PDMA chains in the micelle cores have a diameter of 4.5 nm identical to that of the homo-PDMA in bulk Φ_H LC phase[15] and the semirods are perpendicular to the long axis of the micelles, the cross section of the micelles contains ~11 ($\approx 4.5 \times 2.5$) molecules.

This morphology observation suggests that, most likely, the surface micelles of PEO$_{45}$-*b*-PDMA$_{69}$ are compression induced and are thus close to thermodynamic equilibrium. Initially, the diblock molecules are adsorbed to the air/water interface, wherein the PEO blocks adopt a pancake conformation.[10,12,17] Using the area per monomer of 0.41 nm^2 for the PDMA (estimated from homo-PDMA, see Supporting Information) and 0.27–0.30 nm^2/monomer for the pancake PEO,[10a,17c] the total area of an adsorbed PEO$_{45}$-*b*-PDMA$_{69}$ molecule is calculated as 40–42 nm^2/molecule, close to the A_{ON} in Figure 1. Therefore,

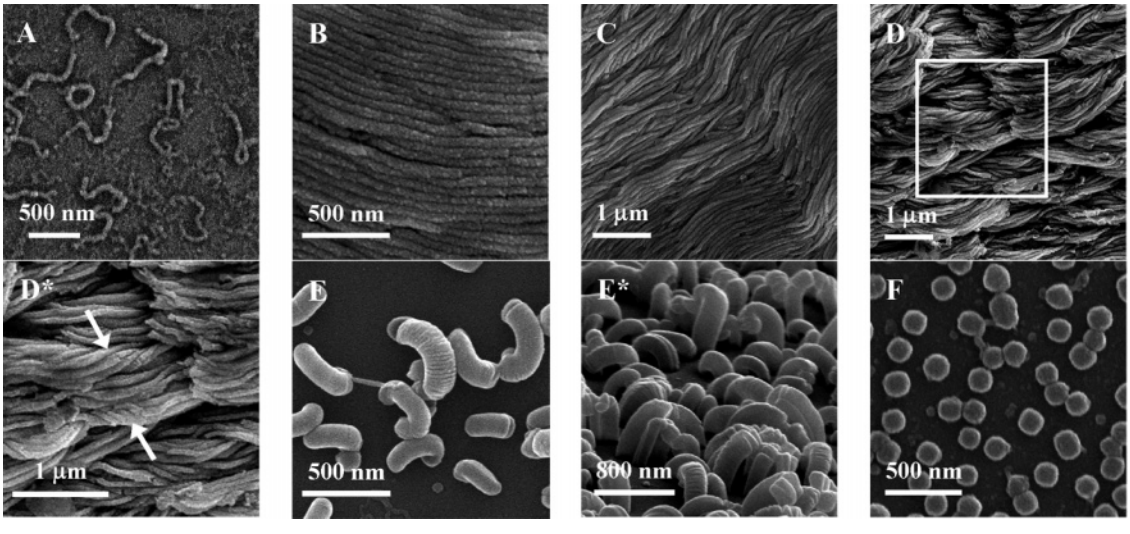

Figure 2. A set of SEM images of the LB films at various molecular areas. The images A–F correspond to the points A–F in Figure 1. D* is the enlarged image of the area indicated by the square in D, where the twisted micelles are pointed by the arrows. E* shows the "springs" at point E with a viewing angle.

at the onset, the air/water interface is nearly fully covered by the adsorbed molecules. The continuous increase in π thereafter will be associated with the PEO desorption, where the PEO conformation changes from pancake to brush. The limiting area of 28.6 nm^2/molecule is consistent to the area occupied by one PDMA block (69 × 0.41 nm^2/momoner = 28.3 nm^2/block), inferring that almost all the diblock molecules have their short PEO chains immersed into the subphase during the first π increase. Meanwhile, the PDMA blocks get close enough to assemble into the cores of the surface micelles, and the PEO blocks form the shells. In our SEM experiments, the EDX microanalysis on the micelle surfae gave a composition of nearly two carbons and one oxygen, matching up to the PEO repeating unit (see Supporting Information).

Figure 2C,D represents two typical morphologies obtained within the plateau region of the isotherm. Obviously, the isotherm plateau of the PEO$_{45}$-*b*-PDMA$_{69}$ is attributed to the packing of the micelles. After the 2D ordered close packing of the micelles appears at A_P, the micelles become bended and broken (Figure 2C at 18 nm^2/molecule) and later twisted and even interwound to bundles (Figure 2D at 14 nm^2/molecule) upon further compression. Of interest is that the micelles can be twisted with both right- and left-handed sense (see Figure 2D*). We suspect that the micelles packed in a parallel fashion are forced to rotate along their long axis with the increased compression, and the friction between the neighboring micelles may cause such a micelle twisting. Recently, we found a triblock copolymer of PDMA$_{43}$-*b*-PEO$_{91}$-*b*-PDMA$_{43}$ self-assembled into cylindrical micelles with a well-defined helical structure in THF/H_2O mixture.[19] The spontaneous formation of twisted cylinders may result from the nonnegligible tacticity of the PDMA and the ability of the Percec-type dendritic groups (and also the polymers) to form supramolecular helical structures.[20] For the same reason, the PDMA blocks in this study may also facilitate the surface micelle twisting. Upon compression, it is possible that the PDMA blocks in the micelle cores are rigidified and become more ordered in packing, leading to the helical structures. However, as induced by compression, the helixes of PEO$_{45}$-*b*-PDMA$_{69}$ are not perfect.

While a dramatic π increase appears on the isotherm after the plateau region, the LB film collapses. Strikingly, instead of featureless collapsed films, Figure 2E at 8 nm^2/molecule and Figure 2F at 5 nm^2/molecule show two types of characteristic 3D aggregates: one is springlike and the other is disklike, which appears before and after the inflection point at 42 mN/m, respectively. Figure 2E* is a side view showing that the "springs" are fornicate with their ends attached to the films at the air/water interface. Since the top view of the fornicate "springs" (Figure 2E) may give thinner projection of the pitches, we estimated the pitch length from the side view of our SEM images (for example, Figure 2E*). The "spring" pitch is around 40 nm, close to the width of the surface micelles, implying that the "springs" arise from the rolled packing of the micelles. The "springs" can result from the tension release of the twisted micelles. As the film is unable to be further subjected to the increased compression, a twisted micelle may have its center part immersed into the subphase and then relax in 3D space, leading to a "spring". The "disks" with lateral dimension of 150−200 nm (see Figure 2F) and the height of 50−150 nm (estimated from our side view images) seem to be compact. We suspect that at the final stage the compression can squeeze the "springs" to chuck out the space therein. The micelles then collapse and even fuse together to form "disks".

In summary, we have investigated the interfacial behavior of a novel ABC of PEO$_{45}$-*b*-PDMA$_{69}$ at various compression stages by the LB balance and morphology study. Accompanied by a pancake-to-brush transition of PEO conformation, the wormlike surface micelles are compression induced. The micelles as the building blocks can be arrayed parallel to generate a long-range ordered structure, further bended and twisted upon compression. Unusual 3D large aggregates of "springs" and "disks" appear when the LB film completely collapses. Such a rich phenomenon of hierarchical nanostructure evolution should be attributed to the coil−semirod architecture of the diblock and the unique assembly ability of the Percec-type dendronized PDMA. This provides a clue in designing block copolymers to control the nanostructures at the air/water interface.

Acknowledgment. This work was financially supported by National Natural Science Foundation of China (50273042, 20025414, and 50573001), the Fund of Polymer Chemistry Laboratory, Chinese Academy of Science and China Petro-Chemical Corp. We also thank Prof. A. D. Schlüter and Prof. A. -F. Zhang for their constructive and valuable suggestions.

Supporting Information Available: The synthesis and molecular characterization of PEO$_{45}$-*b*-PDMA$_{69}$, the surface pressure−area isotherm of the homo-PDMA$_{29}$, and the EDX microanalysis result. This material is available free of charge via the Internet at http://pubs.acs.org.

References and Notes

(1) Halperin, A.; Tirrell, M.; Lodge, T. P. *Adv. Polym. Sci.* **1992**, *100*, 31.

(2) Förster, S.; Antonietti, M. *Adv. Mater.* **1998**, *10*, 195.

(3) Förster, S.; Plantenberg, T. *Angew. Chem., Int. Ed.* **2002**, *41*, 688.

(4) Riess, G. *Prog. Polym. Sci.* **2003**, *28*, 1107.

(5) Cox, J. K.; Eisenberg, A.; Lennox, R. B. *Curr. Opin. Colloid Interface Sci.* **1999**, *4*, 52.

(6) (a) Zhu, J.; Eisenberg, A.; Lennox, R. B. *J. Am. Chem. Soc.* **1991**, *113*, 5583. (b) Li, S.; Hanley, S.; Khan, I.; Varshney, S. K.; Eisenberg, A.; Lennox, R. B. *Langmuir* **1993**, *9*, 2243.

(7) (a) Zhu, J.; Lennox, R. B.; Eisenberg, A. *J. Phys. Chem.* **1992**, *96*, 4727. (b) Zhu, J.; Eisenberg, A.; Lennox, R. B. *Macromolecules* **1992**, *25*, 6547.

(8) Israelachvili, J. *Langmuir* **1994**, *10*, 3774.

(9) (a) An, S. W.; Su, T. J.; Thomas, R. K.; Baines, F. L.; Billingham, N. C.; Armes, S. P.; Penfold, J. *J. Phys. Chem. B* **1998**, *102*, 387. (b) Seo, Y.; Im, J. H.; Lee, J. S.; Kim, J. H. *Macromolecules* **2001**, *34*, 4842. (c) Seo, Y.; Paeng, K.; Park, S. *Macromolecules* **2001**, *34*, 8735. (d) Seo, Y.; Esker, A. R.; Sohn, D.; Kim, H. J.; Park, S.; Yu, H. *Langmuir* **2003**, *19*, 3313. (e) Peleshanko, S.; Gunawidjaja, R.; Jeong, J.; Shevchenko, V. V.; Tsukruk, V. V. *Langmuir* **2004**, *20*, 9423.

(10) (a) Baker, S. M.; Leach, K. A.; Devereaux, C. E.; Gragson, D. E. *Macromolecules* **2000**, *33*, 5432. (b) Devereaux, C. E.; Baker, S. M. *Macromolecules* **2002**, *35*, 1921. (c) Hosoi, A. E.; Kogan, D.; Devereaux, C. E.; Bernoff, A. J.; Baker, S. M. *Phys. Rev. Lett.* **2005**, *95*, 037801.

(11) (a) Zhu, J.; Eisenberg, A.; Lennox, R. B. *Macromolecules* **1992**, *25*, 6556. (b) Meszaros, M.; Eisenberg, A.; Lennox, R. B. *Faraday Discuss.* **1994**, *98*, 283. (c) Li, S.; Clarke, C. J.; Lennox, R. B.; Eisenberg, A. *Colloids Surf., A* **1998**, *133*, 191. (d) Cox, J. K.; Yu, K.; Constanine, B.; Eisenberg, A.; Lennox, R. B. *Langmuir* **1999**, *15*, 7714.

(12) Logan, J. L.; Masse, P.; Dorvel, B.; Skolnik, A. M.; Sheiko, S. S.; Francis, R.; Taton, D.; Gnanou, Y.; Duran, R. S. *Langmuir* **2005**, *21*, 3424.

(13) Kim, Y.; Pyun, J.; Fréchet, J. M. J.; Hawker, C. J.; Frank, C. W. *Langmuir* **2005**, *21*, 10444.

(14) (a) Ober, C. K. *Science* **2000**, *288*, 448. (b) Karakaya, B.; Claussen, W.; Gessler, K.; Saenger, W.; Schlüter, A. D. *J. Am. Chem. Soc.* **1997**, *119*, 3296. (c) Schlüter, A. D.; Rabe, J. P. *Angew. Chem., Int. Ed.* **2000**, *39*, 864. (d) Percec, V.; Glodde, M.; Bera, T. M.; Miura, Y.; Shiyanovskaya, I.; Singer, K. D.; Balagurusamy, V. S. K.; Heiney, P. A.; Schnell, I.; Rapp, A.; Spiess, H.-W.; Hudson, S. D.; Duan, H.

Nature (London) **2002**, *419*, 384. (e) Frauenrath, H. *Prog. Polym. Sci.* **2005**, *30*, 325.

(15) Percec, V.; Ahn, C.-H.; Cho, W.-D.; Jamieson, A. M.; Kim, J.; Leman, T.; Schmidt, M.; Gerle, M.; Möller, M.; Prokhorova, S. A.; Sheiko, S. S.; Cheng, S. Z. D.; Zhang, A.; Ungar, G.; Yeardley, D. J. P. *J. Am. Chem. Soc.* **1998**, *120*, 8619.

(16) (a) Cheng, C.-X.; Tang, R.-P.; Zhao, Y.-L.; Xi, F. *J. Appl. Polym. Sci.* **2004**, *91*, 2733. (b) Cheng, C.-X.; Tian, Y.; Shi, Y.-Q.; Tang, R.-P.; Xi, F. *Macromol. Rapid Commun.* **2005**, *26*, 1266.

(17) (a) Baekmark, T. R.; Elender, G.; Lasic, D. D.; Sackmann, E. *Langmuir* **1995**, *11*, 3975. (b) Bijsterbosch, H. D.; de Haan, V. O.; de Graaf, A. W.; Mellema, M.; Leermakers, F. A. M.; Cohen Stuart, M. A.; van Well, A. A. *Langmuir* **1995**, *11*, 4467. (c) Goncalves da Silva, A. M.; Filipe, E. J. M.; d'Oliveira, J. M. R.; Martinho, J. M. G. *Langmuir* **1996**, *12*, 6547. (d) Currie, E. P. K.; Leermakers, F. A. M.; Cohen Stuart, M. A.; Fleer, G. J. *Macromolecules* **1999**, *32*, 487. (e) Fauré, M. C.; Bassereau, P.; Lee, L. T.; Menelle, A.; Lheveder, C. *Macromolecules* **1999**, *32*, 8538. (f) Xu, Z.; Holland, N. B.; Marchant, R. E. *Langmuir* **2001**, *17*, 377. (g) Wesemann, A.; Ahrens, H.; Steitz, R.; Förster, S.; Helm, C. A. *Langmuir* **2003**, *19*, 709.

(18) Zhu, J.; Lennox, R. B.; Eisenberg, A. *Langmuir* **1991**, *7*, 1579.

(19) Cheng, C.-X.; Huang, H.; Tang, R.-P.; Chen, E.-Q.; Xi, F. *Macromolecules* **2005**, *38*, 3044.

(20) (a) Kwon, Y. K.; Chvalun, S.; Schneider, A.-I.; Blackwell, J.; Percec, V.; Heck, J. A. *Macromolecules* **1994**, *27*, 6129. (b) Percec, V.; Ahn, C.-H.; Barboiu, B. *J. Am. Chem. Soc.* **1997**, *119*, 12978. (c) Percec, V.; Dulcey, A. E.; Balagurusamy, V. S. K.; Miura, Y.; Smidrkal, J.; Peterca, M.; Nummelin, S.; Edlund, U.; Hudson, S. D.; Heiney, P. A.; Duan, H.; Magonov, S. N.; Vinogradov, S. A. *Nature (London)* **2004**, *430*, 764.

MA0614500